2014 IEEE International Conference on Robotics & Automation (ICRA)
Hong Kong Convention and Exhibition Center
May 31 - June 7, 2014. Hong Kong, China

A Novel Tumor Localization Method using Haptic Palpation Based on Soft Tissue Probing Data

Min Li, Angela Faragasso, Jelizavata Konstantinova, Vahid Aminzadeh, Lakmal D. Seneviratne, *Member, IEEE,* Prokar Dasgupta, Kaspar Althoefer, *Member, IEEE*

Abstract— **Current surgical tele-manipulators do not provide explicit haptic feedback during soft tissue palpation. Haptic information could improve the clinical outcomes significantly and help to detect hard inclusions within soft-tissue organs indicating potential abnormalities. However, system instability is often caught by direct force feedback. In this paper, a new approach to intra-operative tumor localization is introduced. A virtual-environment tissue model is created based on the reconstructed surface of a soft-tissue organ using a Kinect depth sensor and the organ's stiffness distribution acquired during rolling indentation measurements. Palpation applied to this tissue model is haptically fed back to the user. In contrast to previous work, our method avoids the control issues inherent to systems that provide direct force feedback. We demonstrate the feasibility of this method by evaluating the performance of our tumor localization method on a soft tissue phantom containing buried stiff nodules. Results show that participants can identify the embedded tumors; the proposed method performed nearly as well as manual palpation.**

I. Introduction

Palpation is a process where a clinician examines soft tissue organs during open surgery with their fingers to detect abnormalities beneath the surface [1]. Intra-operative palpation is a widely-used procedure to identify abnormal tissue regions [2]. Information of spatially distributed tissue stiffness is essential for palpation. Areas that are stiffer than the surrounding tissue are recognized as possible tumors [3]. During open surgery, which is carried out using a single large incision, intra-operative palpation is easily conducted by the surgeons using their hands. Robot-assisted Minimally Invasive Surgery (RMIS) has been widely applied in recent years. However, the physical contact between the surgeon and the soft tissue is cut off, which makes palpation and tumor identification difficult [4].

Providing direct force feedback enables palpation via a surgical tele-manipulator [5]. However, most existing robotic surgical systems, such as da Vinci and Titan Medical Amadeus, do not provide haptic feedback. Only DLR (German Aerospace Center) has created a 7 DOF robotic system for surgery providing bimanual force feedback and 3D vision [6]. Two input devices Sigma.7 are used at the master side for manipulation and force feedback. Bilateral tele-operation controllers are popular in multi-DOF haptic feedback surgery robot research [5], [7]. This approach makes use of a four-channel architecture for tele-operation control considering forces both from the master and slave, as well as the position difference between the master and the slave. However, with the increase of the system's transparency, instability caused by jitters generated from small delays and errors in the system often leads to unacceptable oscillation at the master and the slave side during surgery. The trade-off between transparency (matching level of the feedback forces and the forces applied at the tool tip) and system stability is a limitation of direct force feedback [8].

Alternatively, a graphical display of the organ's stiffness distribution can be used to show the locations of tumors to surgeons [9-11]. Liu et al. [9] proposed a rolling indentation tissue probing approach to localize abnormalities during MIS; the stiffness distribution map of a soft tissue surface can be generated by exposing the tissue surface to continuous rolling indentation using a force-sensitive wheeled probe. However, a disadvantage of this method is that the colors of the resultant stiffness maps can only represent relative stiffness values [11]. Even if the magnitude of stiffness were provided, it is still difficult for surgeons to form an impression of the actual tissue stiffness at different points of the organ.

Commonly, palpation simulators provide graphical feedback of the deformable tissue through computer graphics and force feedback via a haptic device. To generate haptic cues of virtual objects, motion tracking, collision detection between the virtual fingertip and the virtual objects, calculation of the reaction forces are required; relaying the resultant reaction forces to the user closes the loop to achieve a complete haptic feedback system. A deformable soft tissue model is often used to concurrently compute tissue deformation and reaction forces as a function of indentation depth and palpation velocity. Mahvash et al. [12] pointed out that if real-time intra-operative tissue models can be created, a force display could be based on this model rather than the on-line measured force. Thus, haptic palpation in RMIS can benefit from palpation simulation systems. There are some early attempts applying palpation simulation to intra-operative soft tissue tumor localization in RMIS by using estimated soft tissue parameters. For example, Khaled et al. [13] reconstructed virtual objects based on the results of real-time ultrasound elastography.

M. Li, A. Faragasso, J. Konstantinova, V. Aminzadeh, L. D. Seneviratne and K. Althoefer are with the Department of Informatics, Kings College London, U.K. (e-mail: {min.m.li; angela.faragasso; jelizaveta.zirjakova; vahid.aminzadeh; lakmal.seneviratne; k.althoefer}@kcl.ac.uk).

L. D. Seneviratne is with College of Engineering, Khalifa University of Science, Technology and Research, Abu Dhabi, U.A.E. (e-mail: lakmal.seneviratne@kustar.ac.ae).

P. Dasgupta is with MRC Centre for Transplantation, DTIMB and NIHR BRC, King's College London (e-mail: prokar.dasgupta@kcl.ac.uk).

In this paper, a novel tumor localization method providing force feedback utilizing real-time tissue models is introduced and validated. A tissue model is created in a virtual environment based on the reconstructed surface obtained using a Kinect depth sensor and the model's stiffness distribution is acquired from rolling indentation experiments on a phantom tissue sample. With the generated tissue model, the user can explore the stiffness distribution independently of the real tissue. This method avoids the control issues linked to direct force feedback. Also, the user receives a sense of touch through force feedback instead of relying on relative stiffness differences values provided by a graphical display. The concept of this method is presented in Section II; Section III presents the process of the tissue model creation; Section IV depicts the feedback to the user; Section V shows human-subject palpation experiments on the tissue model using force feedbacks and tissue deformation visual feedback; Section VI draws out conclusions.

II. Method Concept

Fig. 1 depicts the flow chart of the validation test of the concept of our method. First, a soft tissue model is generated from parameters of a tissue sample using a depth sensor and a rolling indentation probe. The tissue surface is reconstructed from the stereoscopic image acquired from the depth sensor. Then the reaction force is measured by using a force sensor attached on a rolling indentation probe. A rolling indentation trajectory with a certain indentation depth can be generated based on the reconstructed tissue surface coordinates. Next, a robot arm is programmed to conduct the rolling indentation following the trajectory. During the indentation probing, indentation depth/reaction force pairs are obtained enabling tissue stiffness distribution acquisition. The reconstructed tissue surface is used to ensure that the indentation depth during the rolling indentation is kept constant. A force distribution matrix can be obtained, which represents the tissue's elastic modulus distribution at a given indentation depth; we assume that the investigated tissue is isotropic, homogeneous, and incompressible [14], [15]. A force distribution matrix can be obtained for each indentation depth; groups of indentation depth/force pairs at different tissue points can be generated. A soft tissue model is then established based on the reconstructed tissue surface and tissue stiffness distribution. A geometrical deformable soft tissue model is employed to visualize the tissue deformation. Unlike the commonly used mass spring based models in virtual reality-based simulations, the influence of the indenter diameter on tissue deformation is considered in this geometrical deformable soft tissue model. The force calculation is based on a look-up table and linear interpolation of measured indentation depth/force pairs during rolling indentation. Since the rolling friction is relatively low compared to the normal reaction force [9], the rolling friction is ignored, assuming that the contact between the indenter and soft tissue as "frictionless". Thus, the virtual tissue can be palpated with real-time tissue deformation and force feedback.

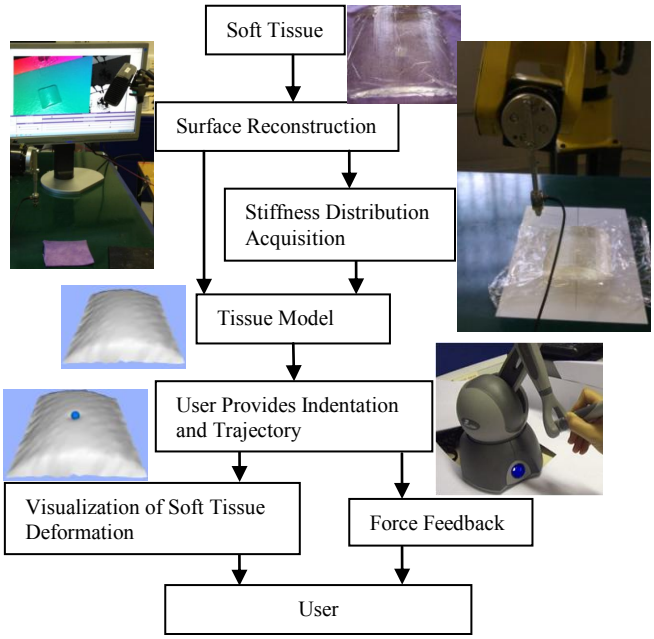

Figure 1. Flowchart of tumor localization using a data-driven tissue model

III. Creation of the Tissue Model

A. Phantom Tissue

A silicone phantom tissue (see Fig. 2) is used for the experimental study. A phantom tissue sample with a curved surface contains two embedded spherical nodules (A and B) at a depth of 3 mm, measured from the top of the nodules to the silicone surface. Cancerous formations are typically stiffer compared with healthy soft tissues [16]. According to the 2003 American joint committee on cancer staging, T1 stage tumors are 2 cm or less in greatest dimension [17]. The phantom is fabricated using RTV6166 (TECHSIL Limited, UK) (ratio 4 : 6 and the viscosity 900 mPa·s). The nodules (15 mm in diameter) are made from RTV615 (TECHSIL Limited, UK) (ratio 10:1 and the viscosity 4000 mPa·s).

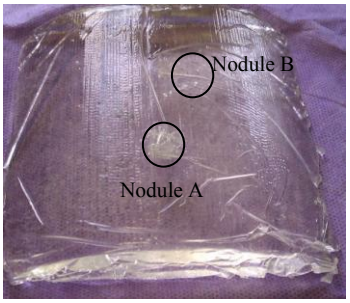

Figure 2. Phantom tissue sample

B. Surface Reconstruction

To obtain real-time intra-operative tissue models, tissue surface reconstruction is required. The objective is to provide a visualized anatomical reconstruction of the soft tissue surface for stiffness distribution acquisition and soft tissue model generation. 3D reconstruction is widely used in many fields including robotics, security, biomedical industries, virtual and augmented reality, and entertainment

[18]. The target is to achieve satisfactory 3D tissue surface reconstruction results without heavy computational effort. Here, a Kinect depth sensor is used. The Kinect depth sensor has been used in many research projects to obtain real-time 3D models of physical scenes. A comparison of the 3D reconstruction produced using the KinectFusion framework with ground truth data obtained from high-precision 3D scanner is given in [19] demonstrating that KinectFusion is a new low-cost solution to resolve object details with a minimum curvature of 10 mm.

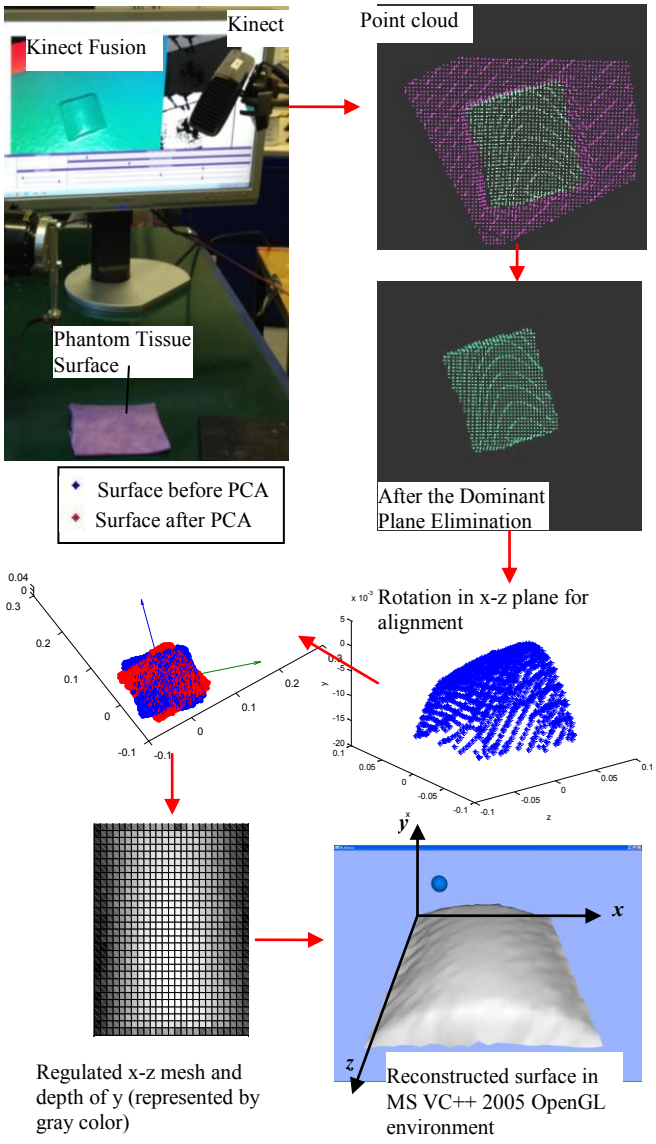

Figure 3. Real-time 3D reconstruction and point cloud processing

Figure 3 shows the real-time tissue surface reconstruction and point cloud processing. Firstly, a real-time 3D reconstruction of the scene was obtained using KinectFusion – this interactive system allowed us to create a single geometrically accurate, high-quality 3D model [20]. A hand-held Kinect sensor was slowly moved around the phantom tissue sample covered by a piece of purple cloth, which was located on a planar table, at about 1 m distance. The 3D model of the scene obtained from the Kinect depth camera was then used to extract the point cloud. Only the point cloud representing the soft tissue surface and the planar table were selected manually cutting off the remaining part of the scene. The plane representing the planar table and the tissue surface were separated using a segmentation program with PCL (Point Cloud Library). The centroid of the points representing the surface is then used to translate the points; the normal of the table plane is used to rotate these points and make them parallel to the x-z plane. Afterwards, the eigenvectors of the covariance matrix are calculated by using a Principal Component Analysis (PCA) transformation, and those eigenvectors were used to rotate the side of the surface and make it parallel to the z axis. Linear interpolation is applied to regulate the points. Finally, the organ surface is reconstructed and displayed on the screen as 1500 small, distributed triangles with 31×26 nodes using OpenGL in VC++. A validation of the tissue surface reconstruction result is provided in Section III C.

C. *Acquisition of Tissue Stiffness Distribution*

At a given and fixed indentation depth, the force distribution matrix obtained using a rolling indentation probe is effectively the tissue's elastic modulus. The results of the tissue surface reconstruction (using the Kinect, as described above) allow us to maintain a constant indentation depth whilst scanning. A robot arm with a rolling indentation probe attached to its end-effecter is programmed to scan the tissue following trajectories maintaining a constant indentation distance from the tissue surface. Whilst the scanning, a set of force matrices are obtained by a force sensor attached to the rolling indentation.

In this paper, an ATI Nano 17 force/torque sensor (SI-12-0.12, resolution 0.003N with 16-bit data acquisition card) and a FANUC robot arm (M-6iB, FANUC Corporation, Japan) are used. The FANUC robot is controlled with FANUC R-J3iC controller (capable of computing the robot's kinematics and dynamics in real time. A sequence of positions from the point cloud are passed into the controller via socket messaging and continuously updated. The controller passes the sequence to its trajectory generator which is set up to work in linear interpolation mode. In this mode of operation, the generated trajectory follows a Hermite interpolation with the following equation,

$$\begin{aligned}\boldsymbol{p}(t) &= \boldsymbol{p}_{ci}(1-3(t_i-t_c)^2t^2+2(t_i-t_c)^3t^3)\\ &+\boldsymbol{p}_{e(i)}(3(t_i-t_c)^2t^2-2(t_i-t_c)^3t^3)\\ &+\alpha(\boldsymbol{p}_{e(i-1)}-\boldsymbol{p}_{ci})(t-2(t_i-t_c)^2t^2+(t_i-t_c)^3t^3)\\ &+\alpha(\boldsymbol{p}_{ci}-\boldsymbol{p}_{e(i-1)})((t_i-t_c)^2t^2+(t_i-t_c)^3t^3)\end{aligned}, \quad (1)$$

where $\boldsymbol{p}_{ei}$ and $\boldsymbol{p}_{e(i-1)}$ are two consecutive points passed to the trajectory generator, $\boldsymbol{p}_{ci}$ is the current location of the robot at the time of the receiving the next position $\boldsymbol{p}_{ei}$ and α is a scalar which determine how strong should the motion of the robot align toward intermediate point. Adjusting scalar parameter α to a high value, the trajectory of the motion of the robot starting from $\boldsymbol{p}_{ci}$ is parallel to the vector $\boldsymbol{p}_{e(i-1)}$- $\boldsymbol{p}_{ci}$ and ends parallel to the vector $\boldsymbol{p}_{ci}$- $\boldsymbol{p}_{e(i-1)}$.

Implementing this method ensures that the robot follows the points as they are passed to it. To avoid any discontinuity of the motion, which could result in varying coefficients of

friction or skipping points, the points are updated when the robot is in close vicinity of the last point. As a result, the point cloud can be followed with continuous motion. Parameter α should be adjusted to reduce motion vibrations as much as possible. Empirical experiments demonstrate best results at α=3.5.

To correctly match the coordinate systems of the robot and the point cloud three points on the robot structure are measured. These points are origin (centroid of the surface) and one point in x and y directions. Based on these points, homogenous transformation matrices are created which transform the points of the point cloud into the robot coordinate frame. To validate the accuracy of the tissue surface reconstruction result, the robot was first programmed to follow the reconstructed tissue surface with an indentation depth of 0. Force data was recorded. The maximum force was 0.041 N. The average force was 0.009 N with a standard deviation of 0.008 N. The result demonstrates the indenter was barely touching the reconstructed surface – hence, following the curvature of the tissue surface accurately during the entire scan process. We conclude that the tissue surface reconstruction can be used for indentation depth control during indentation scans that aim at acquiring a tissue's stiffness distribution. Three rolling indentation process were conducted with the indentation depths of 2 mm, 4 mm and 6 mm. During the process, the soft tissue surface is lubricated. Normal reaction force data was recorded (see Fig. 4). From the force matrices, one can see that the two nodules, A and B, are easily recognizable in the color-coded representation of the force matrix – the two nodules show as high force peaks (distinct red and yellow areas in an otherwise blue (low value) force distribution.

IV. Feedback to the User

A. Visualization of Tissue Deformation

Deformation of the virtual soft tissue during palpation is displayed in real time using a geometrical deformable soft tissue model (see Fig. 5), which was established based on predefined finite element modeling considering the influence of the indenter diameter. The details of this model are presented in [21].

B. Force Feedback

Force feedback is provided via a haptic device (PHANToM Omni from Sensable Technology Inc., see Fig. 1) to enable the user to "palpate" the created tissue model by holding a stylus (described in Section III). The indenter position ($\boldsymbol{P_0}$, the blue sphere in Fig. 5) is acquired and compared with the soft tissue surface continuously. When the tissue surface is contacted by the indenter, the indentation depth is calculated using the distance between the indenter position ($\boldsymbol{P_0}$) and the nearest triangle planar on the mesh of the original tissue surface contour (vertices: $\boldsymbol{P_1}$, $\boldsymbol{P_2}$, $\boldsymbol{P_3}$). The unit normal vector of the planar $\boldsymbol{n}$ is acquired from $(\boldsymbol{P_2}-\boldsymbol{P_1})\times(\boldsymbol{P_3}-\boldsymbol{P_1})/\ ||(\boldsymbol{P_2}-\boldsymbol{P_1})\times(\boldsymbol{P_3}-\boldsymbol{P_1})||$, $\boldsymbol{v}$ is the vector from $\boldsymbol{P_0}$ to $\boldsymbol{P_1}$. This distance is $|\boldsymbol{v}\cdot\boldsymbol{n}|$. According to the calculated indentation depth, the reaction forces are acquired from a look-up table and linear interpolation of measured tissue reaction force matrices of different indentation depths. When the force in the look-up table exceeds the max force (3.3 N) of PHANToM Omni, the force is set to be 3.3 N. Since the surface is lubricated during the rolling indentation process. The tangent force is very small compared with the normal force during the rolling indentation, so it is not fed back to the user. The direction of the normal reaction force (f_n) is defined by a contact normal $\boldsymbol{n}$. The force f_n is decomposed and converted into forces along x, y, z axes of the haptic device (see Fig. 6). Since the reaction force data acquired from rolling indentation with a constant velocity, the proposed haptic palpation approach assumes a constant palpation velocity along the tissue surface and the user needs to palpate with a fairly constant velocity during the experiments.

V. Palpation Experiments

A. Method

An empirical study on the effectiveness of the proposed palpation method, where twenty participants were involved, was carried out (see Table I for the demographics of the involved participants).

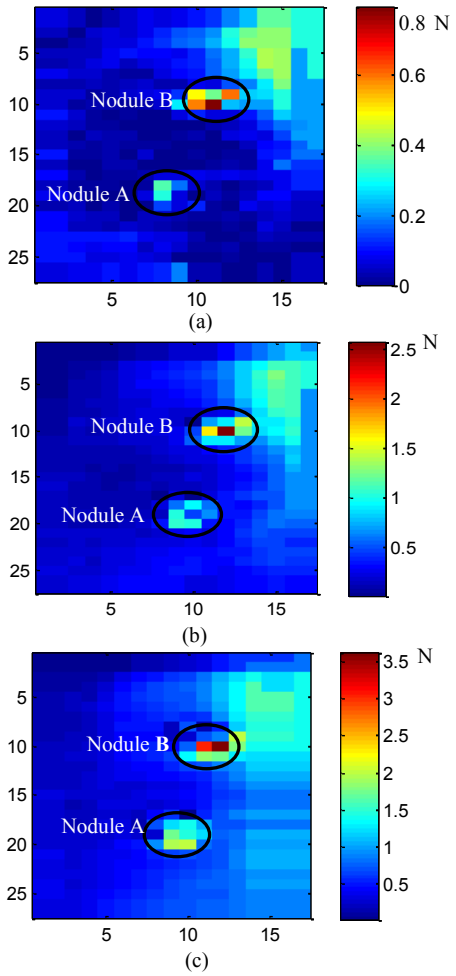

Figure 4. Reaction force matrix at the indentation depth of (a) 2 mm, (b) 4 mm and (c) 6 mm

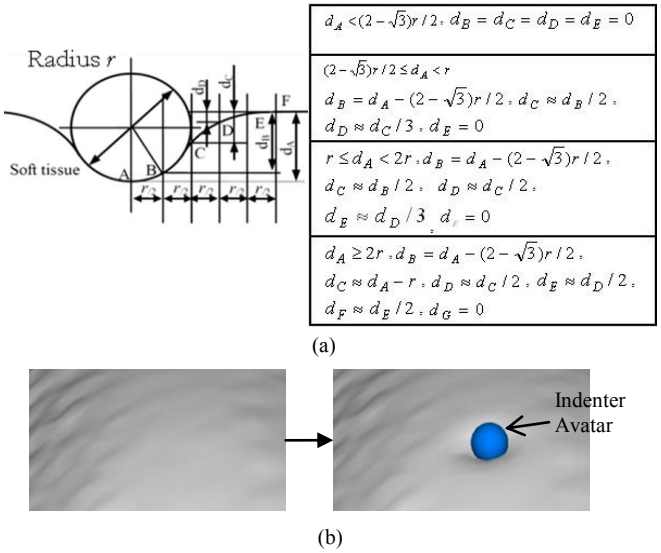

Figure 5. Visualization of tissue deformation: (a) geometrical deformable soft tissue model; (b) tissue deformation result

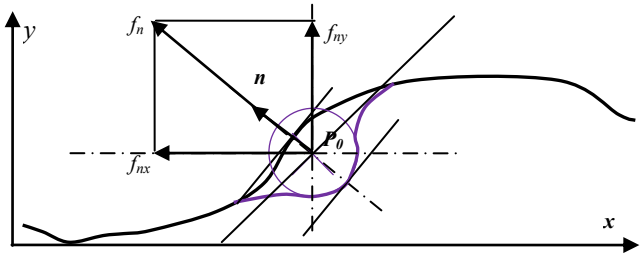

Figure 6. Force direction of haptic feedback

TABLE I. OVERVIEW OF DEMOGRAPHICS AND EXPERIENCE OF THE GROUP

Item	Detail
Age range	19-42
Average age	29.6
Gender	♀: 5; ♂: 15
Handedness	R: 19; L: 1
Palpation experience	1
Engineering background	19
VR simulator	0

Two tests were conducted: manual palpation employing a silicone slab with embedded nodules and haptic palpation with force feedback using the soft tissue model generated based on the surface reconstruction and the stiffness distribution results (described in Section III). To avoid learning effect which might have biased the results in favor of the last test, the order of the two tests was balanced during the experiment. Before the manual palpation experiment, participants were asked to do a practice trial run palpating a transparent silicone phantom tissue with and without nodules inside. During the manual palpation experiment, participants were asked to manually palpate the silicone phantom tissue which was covered by a purple cloth hiding hard nodules buried inside the silicone phantom. The task of this experiment was to find the location of the buried nodules just employing the sense of touch. Before the haptic palpation test, participants were asked to do a practice run with hard nodules that were visible. During the haptic palpation experiment, participants were asked to palpate the virtual tissue with no hidden nodules and to pinpoint the found nodule positions.

B. Results and Discussion

During the two palpation experiments, all participants found the two embedded nodules (Nodule A: 100%; Nodule B: 100%). It is noted that one participant wrongly identified two additional regions as tissue regions where nodules were buried (see the yellow circles in Fig. 7). Localization accuracy is comparable between the haptic palpation and manual palpation. The average time of the manual palpation experiment was 29.15 s (Standard Error = 2.54 s) while the average time of the haptic palpation was 39.95 s (Standard Error = 4.18 s). A Mann-Whitney *U*-test [22] was conducted to compare the consumed time of these two methods. No significant difference was found ($U = 133$, $p = 0.071 > 0.05$). In this experiment, haptic palpation could be seen as efficient as manual palpation.

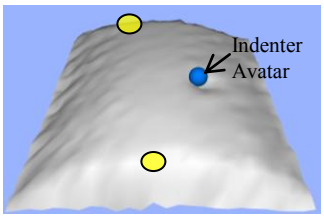

Figure 7. Wrongly recognized hard areas (two yellow circles)

For this method to be employed in a real MIS setting, a smaller and sterilizable depth sensor or a binocular camera would need to be used instead of the Kinect. The two wrongly recognized nodule locations are both at the edges of the tissue model. The reason could be that the particular participant confused the changes of force caused by stiffness differences and the tissue texture. By just observing reaction force maps (like the one shown in Fig. 4), there is a risk of making mistakes in nodule identification and localization. In Fig. 4, there is an area with a relative high reaction force (see top right yellow area in Fig. 4 (a), (b) and (c)), which could be wrongly interpreted as a hard nodule if only the color coding of the shown force matrix was used in the analysis. In our human subject palpation experiments, users were able to detect the hard nodules correctly with the help of force feedback information. The reason for the slightly lower performance during the haptic palpation experiments compared to the manual palpation performance may be related to the limited tactile information experienced during the haptic feedback experiments.

For the proposed 3D tissue surface reconstruction method to be employed in a real MIS setting, a smaller and sterilizable depth sensor or a binocular camera should be used instead of the Kinect. Although there is no official announcement, Microsoft is developing miniaturized Kinect depth sensor, which will be more suitable for the size requirements of MIS tools. Hopefully in the near future, it can be applied in a real MIS setting. In this proposed method, a flat table surface was used to work as a reference planar to segment and rotate the tissue surface and a centroid of tissue surface was used to register the reconstructed tissue

surface to the coordinate frame of the robot. In practice, the tissue will not be sitting on a planar surface in-vivo, but rather on and surrounded by other organs. The proposed method needs to be adapted to those conditions. Manually inserted markers or pins would be one solution. Attach the depth sensor to the surgical robot to unify the coordinate systems would be another solution.

VI. Conclusions

Providing direct force feedback to enable palpation via a surgical tele-manipulator can lead to system instability issues; using tissue stiffness distribution information provided by a graphical display it is difficult for surgeons to form a reliable impression of the actual tissue stiffness. To fill the research gap, an intra-operative tumor localization method providing force feedback utilizing real-time intra-operative tissue models is introduced. Instead of using empirical tissue model parameters, the tissue model in this method represents the properties of investigated soft tissue. A validation test of the concept was conducted by evaluating the performance of the tumor localization on a soft tissue phantom containing buried stiff nodules. The proposed haptic palpation method performed well– although it was noted to be slower than manual palpation. The results revealed that although manual palpation was shown to be less time consuming, the two methods had no significant difference, concerning the nodule identification result. The proposed method avoids the control issues associated with direct force feedback. We demonstrated the potential of our palpation method in medical training, however, a lot of work and effort and user studies remain to show how that this technique can be efficiently used in a real medical training, RMIS and remotely guided open surgery.

Acknowledgment

The work described in this paper is partially funded by the Seventh Framework Programme of the European Commission under grant agreement 287728 in the framework of EU project STIFF-FLOP, by the China Scholarship Council, as well as by the National Institute for Health Research (NIHR) Biomedical Research Centre based at Guy's and St Thomas' NHS Foundation Trust and King's College London. The views expressed are those of the authors and not necessarily those of the NHS, the NIHR or the Department of Health.

References

[1] T. R. Coles, D. Meglan, and N. W. John, "The Role of Haptics in Medical Training Simulators: A Survey of the State of the Art," *IEEE Trans. Haptics*, vol. 4, no. 1, pp. 51–66, Jan. 2011.

[2] M. Nakao, T. Kuroda, M. Komori, and H. Oyama, "Evaluation and user study of haptic simulator for learning palpation in cardiovascular surgery," *Int. Conf. Artif. Real. Telexistence*, pp. 203–208, 2003.

[3] G. De Gersem, "Reliable and enhanced stiffness perception in soft-tissue telemanipulation," *Int. J. Rob. Res.*, vol. 24, no. 10, pp. 805–822, Oct. 2005.

[4] J. C. Gwilliam, Z. Pezzementi, E. Jantho, A. M. Okamura, and S. Hsiao, "Human vs. robotic tactile sensing: Detecting lumps in soft tissue," *2010 IEEE Haptics Symp.*, pp. 21–28, Mar. 2010.

[5] M. Tavakoli, A. Aziminejad, R. V Patel, and M. Moallem, "Methods and mechanisms for contact feedback in a robot-assisted minimally invasive environment.," *Surg. Endosc.*, vol. 20, no. 10, pp. 1570–1579, Oct. 2006.

[6] R. Konietschke, U. Hagn, M. Nickl, S. Jorg, A. Tobergte, G. Passig, U. Seibold, L. Le-Tien, B. Kubler, M. Groger, F. Frohlich, C. Rink, A. Albu-Schaffer, M. Grebenstein, T. Ortmaier, and G. Hirzinger, "The DLR MiroSurge - A robotic system for surgery," in *Proceedings of the IEEE International Conference on Robotics and Automation (2009)*, 2009, pp. 1589–1590.

[7] H. Tanaka, K. Ohnishi, H. Nishi, T. Kawai, Y. Morikawa, S. Ozawa, and T. Furukawa, "Implementation of Bilateral Control System Based on Acceleration Control Using FPGA for Multi-DOF Haptic Endoscopic Surgery Robot," *IEEE Trans. Ind. Electron.*, vol. 56, no. 3, pp. 618–627, 2009.

[8] A. M. Okamura, "Haptic feedback in robot-assisted minimally invasive surgery," *Curr. Opin. Urol.*, vol. 19, no. 1, p. 102, 2009.

[9] H. Liu, D. P. Noonan, B. J. Challacombe, P. Dasgupta, L. D. Seneviratne, and K. Althoefer, "Rolling mechanical imaging for tissue abnormality localization during minimally invasive surgery.," *IEEE Trans. Biomed. Eng.*, vol. 57, no. 2, pp. 404–14, Feb. 2010.

[10] T. Yamamoto and N. Abolhassani, "Augmented reality and haptic interfaces for robot- assisted surgery," *Int. J. Med. Robot. Comput. Assist. Surg.*, vol. 8, no. November 2011, pp. 45–56, 2012.

[11] A. P. Miller, W. J. Peine, J. S. Son, and M. D. Z. T. Hammoud, "Tactile imaging system for localizing Lung nodules during video assisted thoracoscopic surgery," *Proc. 2007 IEEE Int. Conf. Robot. Autom.*, pp. 2996–3001, Apr. 2007.

[12] M. Mahvash, J. Gwilliam, R. Agarwal, B. Vagvolgyi, L.-M. Su, D. D. Yuh, and A. M. Okamura, "Force-Feedback Surgical Teleoperator: Controller Design and Palpation Experiments," *2008 Symp. Haptic Interfaces Virtual Environ. Teleoperator Syst.*, no. Figure 1, pp. 465–471, Mar. 2008.

[13] W. Khaled, S. Reichling, O. T. Bruhns, H. Boese, M. Baumann, G. Monkman, S. Egersdoerfer, D. Klein, A. Tunayar, H. Freimuth, A. Lorenz, A. Pessavento, and H. Ermert, "Palpation imaging using a haptic system for virtual reality applications in medicine," *Stud. Health Technol. Inform.*, vol. 98, pp. 147–153, Jan. 2004.

[14] H. Liu, J. Li, X. Song, L. D. Seneviratne, and K. Althoefer, "Rolling Indentation Probe for Tissue Abnormality Identification During Minimally Invasive Surgery," *IEEE Trans. Robot.*, vol. 27, no. 3, pp. 450–460, 2011.

[15] K. Sangpradit, H. Liu, L. D. Seneviratne, and K. A. Althoefer, "Tissue identification using inverse finite element analysis of rolling indentationof Rolling Indentation," in *IEEE International conference on Robotics and Automation ICRA*, 2009, pp. 1250–1255.

[16] P. Wellman and R. Howe, "Breast tissue stiffness in compression is correlated to histological diagnosis," 1999.

[17] W. a Woodward, E. a Strom, S. L. Tucker, M. D. McNeese, G. H. Perkins, N. R. Schechter, S. E. Singletary, R. L. Theriault, G. N. Hortobagyi, K. K. Hunt, and T. a Buchholz, "Changes in the 2003 American Joint Committee on Cancer staging for breast cancer dramatically affect stage-specific survival.," *J. Clin. Oncol. Off. J. Am. Soc. Clin. Oncol.*, vol. 21, no. 17, pp. 3244–8, Sep. 2003.

[18] G. Kordelas, "State-of-the-art Algorithms for Complete 3D Model Reconstruction," in in *Lecture Notes in Computer Science*, 2010, pp. 1–15.

[19] S. Meister and S. Izadi, "When can we use KinectFusion for ground truth acquisition?," in *Workshop on Color-Depth Camera Fusion in Robotics, IROS*, 2012, pp. 3–8.

[20] S. Izadi, D. Kim, O. Hilliges, D. Molyneaux, R. Newcombe, P. Kohli, J. Shotton, S. Hodges, D. Freeman, A. Davison, and A. Fitzgibbon, "KinectFusion: Real-time 3D Reconstruction and Interaction Using a Moving Depth Camera," in *The ACM Symposium on User Interface Software and Technology (UIST)*, 2011, pp. 559–568.

[21] M. Li, L. D. Seneviratne, P. Dasgupta, and K. A. Althoefer, "Virtual palpation system," in *International Conference on Intelligent Robots and Systems workshop "Learning and Interaction in Haptic Robots,"* 2012.

[22] H. B. Mann and D. R. Whitney, "On a test of whether on of two random variables is stochastically larger than the other," *Ann. Math. Stat.*, vol. 18, no. 1, pp. 50–60, 1947.